

# Lab on a Chip

Accepted Manuscript



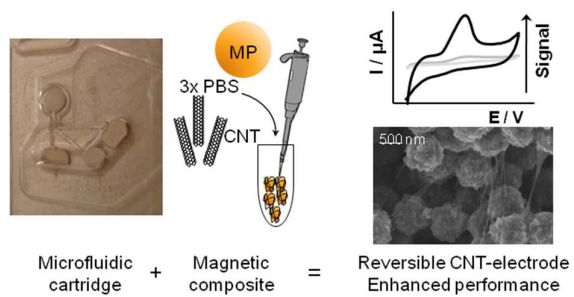
This is an *Accepted Manuscript*, which has been through the Royal Society of Chemistry peer review process and has been accepted for publication.

*Accepted Manuscripts* are published online shortly after acceptance, before technical editing, formatting and proof reading. Using this free service, authors can make their results available to the community, in citable form, before we publish the edited article. We will replace this *Accepted Manuscript* with the edited and formatted *Advance Article* as soon as it is available.

You can find more information about *Accepted Manuscripts* in the [Information for Authors](#).

Please note that technical editing may introduce minor changes to the text and/or graphics, which may alter content. The journal's standard [Terms & Conditions](#) and the [Ethical guidelines](#) still apply. In no event shall the Royal Society of Chemistry be held responsible for any errors or omissions in this *Accepted Manuscript* or any consequences arising from the use of any information it contains.

## TABLE OF CONTENTS ENTRY



A fast and simple method for the reversible nanostructuring of microfluidic electrode devices *in-situ* is reported.

Cite this: DOI: 10.1039/c0xx00000x

www.rsc.org/xxxxxx

## TECHNICAL INNOVATION

**Reversible nanostructuring of microfluidic electrode devices by CNT magnetic co-entrapment**Zorione Herrasti,<sup>a</sup> Fernando Martínez<sup>a</sup> and Eva Baldrich<sup>\*b,c</sup>

Received (in XXX, XXX) Xth XXXXXXXXX 20XX, Accepted Xth XXXXXXXXX 20XX

DOI: 10.1039/b000000x

Carbon nanotubes (CNT) have been extensively used to produce electrodes of enhanced performance but only very recently exploited in microfluidic devices. In these cases, CNT-electrodes had to be produced previous to device assembly, which might damage the CNT layer. Here, we show a fast and simple method for the reversible nanostructuring of microfluidic electrode devices *in-situ*. The procedure is based on attachment of single walled CNT (SWCNT) onto the surface of magnetic particles (MP) and magnetic confinement of the MP/SWCNT composite onto the sensor in a two-step process that provided homogeneous coating. As it is shown, subsequent magnet removal allows MP/SWCNT release and electrode reutilization. Compared to most previously described methods, ours is faster, simpler and also reversible.

The modification of electrodes with CNT is a widely used methodology since 2001, when Luo et al. showed how the incorporation of a layer of SWCNT improved the electrochemical properties of a glassy carbon electrode.<sup>1</sup> Since then, lots of research has been devoted to the study of CNT-modified devices, either to better understand the electron transfer kinetics through the layer of CNT<sup>2,3</sup> or to optimize new protocols for the efficient incorporation of CNTs to the electrode surface.<sup>4,5</sup> However, most of the surface modification techniques used so far entail long and complex procedures and/or harsh conditions, and involve irreversible modification of the electrode as well. This is of special importance in the case of microfluidic electrode devices that, once assembled, are less accessible for pre-treatment, modification and/or regeneration than bulk electrodes. This might partly explain why only a percentage of the microfluidic devices reported over the last decade incorporated CNT, even when nanomaterial incorporation to microfluidic chips has been defended to provide faster electron transfer kinetics, lowered detection potentials, better-defined and resolved peaks, enhanced signals, and higher sensitivity and resolution than those obtained using unmodified electrodes for the analysis of many analytes.<sup>6-9</sup> In most of the examples reported, CNT were either drop-casted onto electrodes<sup>10-12</sup> or grown directly onto insulating Si/SiO<sub>2</sub> by chemical vapour deposition (CVD).<sup>13,14</sup> In both cases, it followed assembly of the CNT-electrodes to the other components of the microfluidic device. Attempts to simplify fabrication and produce cheaper gadgets has been based for long on the utilization of polymeric materials such as poly(dimethylsiloxane), polystyrene,

poly(methyl methacrylate), and polycarbonate.<sup>6,7</sup> Since these materials rarely survive the severe temperature and chemical conditions required for CNT growth or incorporation, SWCNT stamping has been reported as a good alternative.<sup>15-17</sup> More recently, CNT casting or filtering on paper chips has been used for the subsequent production of disposable and low-cost paper microfluidic cartridges.<sup>18-20</sup> It is worth noting that all these strategies require that CNT-electrodes are first produced, either onto a physical substrate or on pre-existing electrodes, to be then appropriately aligned and assembled with the rest of the device components. In this way, multicomponent assembly can damage the CNT layer and/or modify the final electrode effective area.

To the best of our knowledge, only two teams have reported on CNT incorporation under flow conditions; this is, inside preassembled microfluidic electrode devices. In the first example, SWCNT were wrapped with thiolated ssDNA. These SWCNT-ssDNA complexes were then flowed into a 250x50 μm PDMS channel, where they self-assembled on the contained gold thin-film electrodes.<sup>21</sup> In the second example, the gold thin-film electrodes were placed inside a 500x250 μm PDMS microchannel, were modified by cysteamine self-assembly and then conjugated to carboxylated SWCNT via EDC carbodiimide chemistry.<sup>22</sup> Both procedures took hours (>12-24 h).

Here, we show a simpler and faster strategy, which allowed, not only modification of electrodes with SWCNT inside a plastic microfluidic cartridge, but also their reversible nanostructuring in order to facilitate device regeneration and reutilization. This protocol is based on CNT magnetic co-entrapment, which had been previously developed for the production of CNT-modified screen printed electrodes (SPE).<sup>23,24</sup> In those works, a SWCNT aqueous suspension was mixed with magnetic microparticles (MP) in the presence of salt. This induced transient destabilization of the SWCNT suspension, which usually results in formation of SWCNT bundles stabilized by van der Waals forces. However, in the presence of the beads, SWCNT destabilization produced random attachment of the tubes to the surface of MP (Fig. 1a). As a result, a MP/SWCNT composite was created that could be confined onto an SPE by using a magnet. Once the electrochemical measurement had been carried out, the magnet was removed, the MP/SWCNT were released by pipetting, and the SPE could be reused. Furthermore, SWCNT wiring allowed also the direct electrochemical sensing of the MP surface, enhancing the signals generated by molecules bound to them such as dopamine and myeloperoxidase.<sup>25-27</sup>

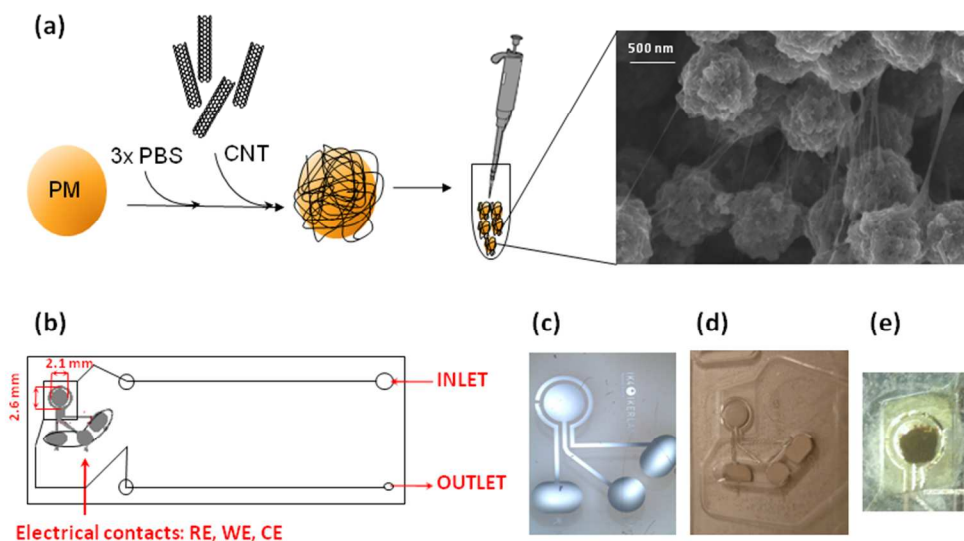


**Fig. 1.** (a) Preparation and SEM image of the MP/SWCNT composite. (b) Scheme of the COP microfluidic cartridge and images of the electrodes (c) before and (d) after cartridge assembly. (e) Amplification of a WE modified with MP/SWCNT in a two-step procedure, as described in the text.

In the present work, this procedure has been successfully re-optimized for the modification of microfluidic thin-film electrode devices *in-situ*, which is the first step towards protocol automation to minimize variability caused by user handling. With this aim, platinum (Pt) thin-film electrodes were produced by standard photolithography on Cyclo Olefin Polymer (COP, 100  $\mu\text{m}$  thick). Briefly, the COP wafer was first cleaned by oxygen plasma and was spin-coated with a positive photoresist (OiR 908-35; Fujifilm). The wafer was then exposed to UV using an acetate mask, was developed, and was submitted to metal sputtering (Pt onto a Ti adhesion layer forming a 145 nm metal film). After lift off in methanol and acetone, the wafer was finally cut to separate the individual chips. For the assembly of the microfluidic cartridge, the COP wafer was vaporized with chlorobenzene and was immediately pressed onto a second COP wafer (1 mm thick) that displayed the microfluidic channels and chamber (Fig. 1b). These were engraved by injection moulding, which was considered the most suitable technique for mass production. Upon assembly, each cartridge was 53.97 mm long and contained a three-electrode detection chamber (5 mm x 4 mm, 10  $\mu\text{L}$  volume) that included working ( $\Phi=2.1$  mm), counter and reference Pt electrodes (Fig. 1c-d). The inlet and outlet channels were 500  $\mu\text{m}$  wide and the distance from the inlet to the electrochemical detection chamber was of 47 mm. The incorporation of Luer connectors enabled the injection of the sample using either a syringe or Luer-Lock caps and a pump, as well as direct pipetting of small volumes. Here, a peristaltic pump P720 (Instech, Plymouth, PA, USA) was connected to the outlet and solutions were flowed through the channel by suction. All the electrochemical measurements were performed using a portable potentiostat designed and developed in IK4-Ikerlan.<sup>28</sup> This equipment includes a specially designed connector port, to which the cartridge was directly plugged without the need for additional cables or adapters. Before its utilization, each sensor was electrochemically activated. For that, the device was filled with PBS (20  $\mu\text{L}$ , 89  $\mu\text{L min}^{-1}$ ), the flow was stopped and 3 pulses of 5 s each were applied at -1.2 V, 0 V and 1.2 V. The electrodes were next characterized by cyclic voltammetry (CV) in ferrocyanide 5

mM and washed again (40  $\mu\text{L}$  of PBS, 89  $\mu\text{L min}^{-1}$ ).

For electrode nanostructuration, carboxylated SWCNT were sonicated in water (1 mg  $\text{mL}^{-1}$ ) for 1 h and 30 min. In order to prevent heating, the water in the tank of the ultrasonic bath was refreshed every 15 min. The composite material was next assembled by mixing in an Eppendorf equal volumes of SWCNT and MP (5 mg  $\text{mL}^{-1}$ ) and adding 3 times concentrated PBS. In the presence of salt, SWCNT suffered transient destabilization and formed bundles that randomly adsorbed onto the surface of MP (Fig. 1a). As a result, blackish aggregates formed that could be observed by the naked eye. These MP/SWCNT complexes were then immediately injected into the cartridge for their magnetic confinement onto the working electrode.

Noteworthy, if a magnet was placed below the working electrode (WE) while the mixture MP/SWCNT was injected, only a proportion of the magnetic composite was retained onto the WE and part of the sediment flowed downstream. This resulted in partial and even nanostructuration of the electrode surface. The best electrode coating was obtained if the modification was performed in two consecutive steps instead, using two neodymium magnets of different size (magnetization N45; Supermagnete, Spain). First, a magnet ( $\Phi=5$  mm, 1 mm high) was placed over the detection chamber. Hence, when the MP/SWCNT composite was injected, it was retained on the ceiling of the compartment (at less than 1 mm above the WE, which is the thickness of the whole cartridge). Then, the first magnet was removed and a second magnet ( $\Phi=1$  mm, 1 mm high) was placed immediately below the WE (at 100  $\mu\text{m}$  of it, which is the thickness of the bottom COP wafer). In this way, the MP/SWCNT composite was relocated and concentrated onto the WE surface, where it generated a homogeneous coating (Fig. 1e).

Fig. 2a compares the behaviour of bare and nanostructured devices in a CV obtained in ferrocyanide. MP/SWCNT-electrodes displayed higher peaks than bare Pt electrodes. Once the electrochemical measurement had been carried out, the magnet was removed and the electrochemical sensor was washed with PBS to remove the MP/SWCNT sediment. The device was characterized again in ferrocyanide to confirm that it had recovered its original state and could be submitted to a new

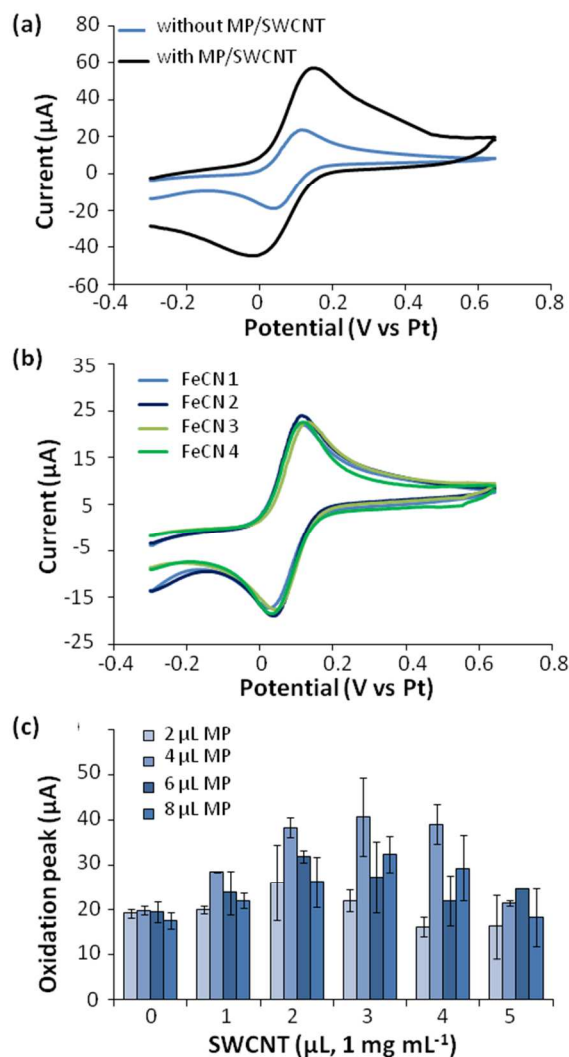


**Fig. 2.** (a) CVs obtained in ferrocyanide 5 mM using either a bare or a nanostructured electrode. (b) Four CV obtained in ferrocyanide using a single microfluidic electrode device before and after 3 consecutive nanostructuring and regeneration rounds. (c) Comparative performance of electrodes modified with increasing amounts of MP and SWCNT.

nanostructuring round. Most microfluidic cartridges ( $n > 20$ ) could be reused in this way at least 4 consecutive times (Fig. 2b). After the fourth consecutive regeneration, some cartridges could not be entirely recovered because traces of MP/SWCNT remained on their surface, and/or they started generating distorted CVs in ferrocyanide. This was attributed to the microfluidic cell design and electrode quality, which limited washing efficiency and electrode reutilization, and should be improved in future.

The MP/SWCNT mixture used for electrode modification was next optimized. Different amounts of MP (2-8  $\mu\text{L}$ , 5  $\text{mg mL}^{-1}$ ) and SWCNT (0- 5  $\mu\text{L}$ , 10  $\text{mg mL}^{-1}$ ) were mixed in parallel with 4  $\mu\text{L}$  of 3x PBS in a final volume of 20  $\mu\text{L}$ , were used to modify the cartridge, and performance was analyzed by CV in ferrocyanide. In all cases, modified electrodes generated higher peaks in the CV than bare Pt electrodes. However, amounts of MP lower than 4  $\mu\text{L}$  were insufficient to cover the surface and support efficient SWCNT wiring. Higher numbers of MP, on the other hand, produced a thick multilayer that was more difficult to remove for electrode reutilization, and generated series of secondary peaks in

the CV that presumably indicated a thin-film effect.<sup>2,3</sup> In relation to the amount of SWCNT used, the peak height registered in the CV increased with the amount of SWCNT added up to 2-3  $\mu\text{L}$  and worsened above 4  $\mu\text{L}$  of SWCNT. In view of this, we selected for subsequent experiments nanostructuring of these electrodes using 4  $\mu\text{L}$  of MP and 3  $\mu\text{L}$  of SWCNT (Fig. 2c).

These nanostructured microfluidic electrode devices were additionally assayed by detecting uric acid (UA). Different concentrations of UA were prepared in PBS and were injected in the cartridge (either bare or nanostructured) at a flow rate of 40  $\mu\text{L min}^{-1}$ . Flow was then stopped and UA was detected by CV. As before, nanostructuring improved detection and SWCNT-modified devices registered narrower peaks that were in average 3-6 fold higher than those observed at bare electrodes (Fig. 3a). While at bare cartridges UA was not detected below 200  $\mu\text{M}$ , nanostructured sensors consistently distinguished concentrations as low as 50  $\mu\text{M}$  and detected 50% of the samples containing 20  $\mu\text{M}$  of UA (Fig. 3b). Furthermore, nanostructuring correlated also with a wider detection range and higher sensitivity (measured as the graph slope; Fig. 3b, insert). It could thus be concluded that the nanostructuring procedure improved significantly the performance of these microfluidic cartridges.

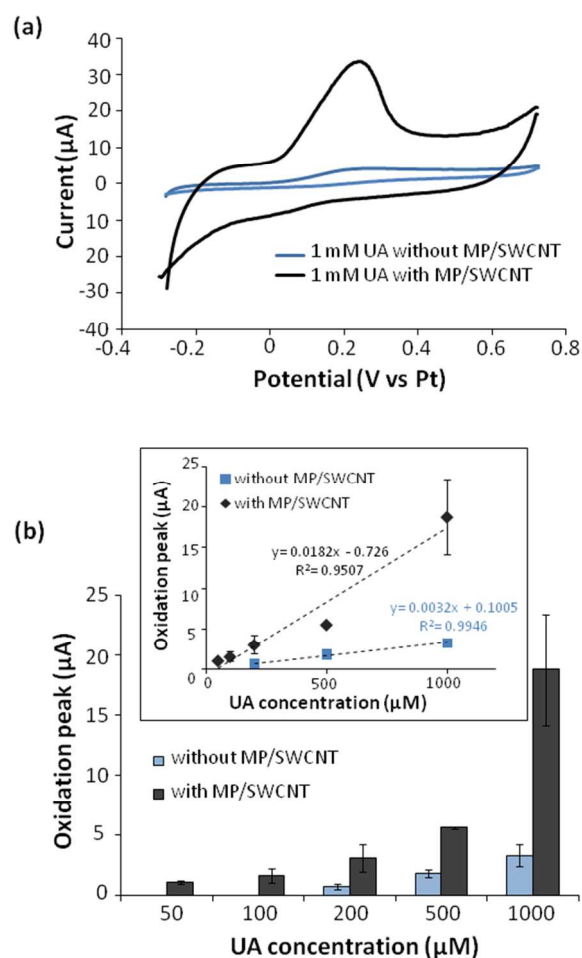


**Fig. 3.** (a) Two CVs obtained in UA 1 mM using either a bare or a nanostructured electrode. (b) Detection of increasing concentrations of UA using either a bare or a nanostructured electrode.

## Conclusions

We have reported on a protocol for the modification of microfluidic electrode devices with SWCNT that, apart from reversible, is significantly simpler and faster than most of the strategies reported previously. Performing electrode nanostructuring in-situ, inside a microfluidic cartridge, should facilitate protocol automation. This could be of interest in many analytical fields, such as diagnostics or detection of reactive analytes, in which a new electrode should be used, but in which reutilization of potentially complex microfluidic platforms could decrease assay cost. Remarkably, the procedure reported could be additionally modified, for instance to produce MP/SWCNT composites that included additional components, such as metal nanoparticles or electroactive polymers, to further ameliorate electrode behaviour or target specific analytes. Nevertheless, the performance of our microfluidic electrode devices, both bare and nanostructured, is still far away from the results reported by other authors for bulk electrodes modified with either CNT or multi-component CNT composites, with claimed limits of detection (LOD) in the high nanomolar to low micromolar range for UA.<sup>29-31</sup> It has been already pointed out by other authors that CV in minute volumes and chambers produce results that deviate from those observed for bulk electrodes in bigger volumes, which was attributed to depletion of redox species and restricted diffusion patterns.<sup>32</sup> Hence, a better design of the microfluidic chamber and optimization of the flow and electrochemical detection conditions might help in future works. Another factor that could be improved is fabrication of electrodes on COP, for instance by producing smaller and more sensitive electrodes or by substituting the Pt pseudoreference by an Ag/AgCl integrated reference electrode. Finally, automation of the mixing, delivery and magnetic confinement of the MP/SWCNT composite should minimize handling by the user and provide more reproducible results.

## Acknowledgements

The authors would like to thank the EU FP7 LABONFOIL project 224306. This work was supported by the Miguel Servet program, grant CP13/00052, which is funded by the Fondo de Investigaciones Sanitarias of the Instituto de Salud Carlos III and cofinanced by the European Regional Development Fund (ERDF).

## Notes and references

<sup>a</sup> IK4-Ikerlan Technological Research Centre, 20500 Mondragón, Spain.  
<sup>b</sup> Diagnostic Nanotools Group. Molecular Biology and Biochemistry Research Center for Nanomedicine (Cibbim-Nanomedicine). Vall d'Hebron Institut de Recerca (VHIR), Universitat Autònoma de Barcelona, Passeig de la Vall d'Hebron 119-129,08035 Barcelona, Spain. E-mail: [eva.baldrich@vhir.org](mailto:eva.baldrich@vhir.org)  
<sup>c</sup> Centro de Investigación Biomédica en Red - Bioingeniería, Biomateriales y Nanomedicina (CIBER-BBN), Spain.

1 H. Luo, Z. Shi, N. Li, Z. Gu and Q. Zhuang, *Anal. Chem.*, 2001, **73**, 915.  
 2 I. Streeter, G.G. Wildgoose, L. Shao and R.G. Compton, *Sens. Act. B*, 2008, **133**, 462.

3 M. Pumera, *Chem. A Europ. J.*, 2009, **15**, 4970.  
 4 P. Yañez-Sedeño, J. Riu, J. M. Pingarron and F. X. Rius, *Trends Anal. Chem.*, 2010, **29**, 939.  
 5 N. Yang, X. Chen, T. Ren, P. Zhang and D. Yang, *Sens. Act. B*, 2015, **207**, 690.  
 6 M. Sierra-Rodero, J. M. Fernández-Romero and A. Gómez-Hens, *Trends Anal. Chem.*, 2014, **57**, 23.  
 7 R. Monosik, L. Angnes, *Microchem. J.*, 2015, **119**, 159.  
 8 M. Pumera, *Chem. Comm.*, 2011, **47**, 5671.  
 9 M. Pumera and A. Escarpa, *Electrophoresis*, 2009, **30**, 3315.  
 10 A.G. Crevillén, M. Pumera, M.C. González and A. Escarpa, *Lab Chip*, 2009, **9**, 346.  
 11 A.G. Crevillén, M. Avila, M. Pumera, M.C. González and A. Escarpa, *Anal. Chem.*, 2007, **79**, 7408.  
 12 M. Pumera, A. Merkoçi and S. Alegret, *Electrophoresis*, 2007, **28**, 1274.  
 13 S. Sansuk, E. Bitziou, M. B. Joseph, J. A. Covington, M. G. Boutelle, P. R. Unwin and J. V. Macpherson, *Anal. Chem.*, 2013, **85**, 163.  
 14 J. Kim, J. Elsnab, C. Gehrke, J. Li and B. K. Gale, *Sens. Act. B*, 2013, **185**, 370.  
 15 J. N. Tey, P. M. Wijaya, Z. Wang, W. H. Goh, A. Palaniappan, S. h. G. Mhaisalkar, I. Rodriguez, S. Dunham and J. A. Rogers, *Appl. Phys. Lett.*, 2009, **94**, 013107.  
 16 D. Vilela, J. Garoz, A. Colina, M.C. González and A. Escarpa, *Anal. Chem.* 2012, **84**, 10838.  
 17 D. Vilela, A. Martin, M. C. Gonzalez, A. Escarpa, *Analyst*, 2014, **139**, 2342.  
 18 P. Wang, L. Ge, M. Yan, X. Song, S. Ge and J. Yu, *Biosens. Bioelectron.*, 2012, **32**, 238.  
 19 K.F. Lei and S.-I. Yang, *J. Nanosci. Nanotech.*, 2013, **13**, 6917.  
 20 K.F. Lei, S.-I. Yang, S.-W. Tsai and H.-T. Hsu, *Talanta*, 2015, **134**, 264.  
 21 F. C. Moraes, R. S. Lima, T. P. Segato, I. Cesarino, J. L. M. Cetino, S. A. S. Machado, F. Gomez and E. Carrilho, *Lab Chip*, 2012, **12**, 1959.  
 22 J. Yu, S. M. Matthews, K. Yunus, J. G. Shapter and A. C. Fisher, *Int. J. Electrochem. Sci.*, 2013, **8**, 1849.  
 23 E. Baldrich, R. Gómez, G. Gabriel and F.X. Muñoz, *Biosens. Bioelectron.*, 2011, **26**, 1876.  
 24 R. Olivé-Monllau, F.X. Muñoz-Pascual and E. Baldrich, *Sens. Act. B*, 2013, **185**, 685.  
 25 E. E. Baldrich and F.X. Muñoz, *Anal. Chem.*, 2011, **83**, 9244.  
 26 Z. Herrasti, F. Martínez and E. Baldrich, *Sens. Act. B*, 2014, **203**, 891.  
 27 Z. Herrasti, F. Martínez and E. Baldrich, *Anal. Bioanal. Chem.*, 2014, **406**, 5487.  
 28 Z. Herrasti, I. Etxabe, J.M. Mitxelena, I. Gabilondo, M.P. Martínez and F. Martínez, *Sens. Act. B*, 2013, **189**, 66.  
 29 S. Wei, F. Zhao and B. Zeng, *Microchim. Acta*, 2005, 150, 219; S. Zhu, H. Li, W. Niu and G. Xu, *Biosens. Bioelectron.*, 2009, **25**, 940.  
 30 H. Zhang, J. Zhang and J. Zheng, *J. Int Meas. Conf.*, 2015, **59**, 177.  
 31 S. He, Y. Yu, Z. Chen, Q. Shi and L. Zhang, *Anal. Lett.*, 2015, **48**, 248.  
 32 T. Li and W. Hu, *Nanoscale*, 2011, **3**, 166.